Monatshefte für Chemie 136, 1853–1860 (2005)
DOI 10.1007/s00706-005-0312-0

Monatshefte für Chemie
Chemical Monthly
Printed in Austria

Modeling of Equilibria in Complex Cryolite Melts[#]

Robert A. Rapp[*] and **Yunshu Zhang**

Department of Materials Science & Engineering, The Ohio State University, Columbus, OH 43210, USA

Received September 12, 2004; accepted November 11, 2004
Published online June 17, 2005

Summary. In the fully ionized sodium sulfate melt, the solubility of an oxide (at a given melt basicity) is well described by considering a single equilibrium to form a specific simple acidic or basic solute. In this case, the dominant solutes are identified by a simple log–log interpretation describing the dependence of the solute concentration on an acid-base parameter ($\log a_{Na_2O}$). However, in fused cryolite (Na_3AlF_6) solutions, the solvent itself and the solutes of oxides involve anionic complexes (alumino-fluorides and oxy-fluorides). Therefore, a single simple equilibrium does not suffice to model the complex solution. Rather, as for a high temperature multi-component gas phase containing many complex volatile species, every possible equilibrium must be individually satisfied and coupled to a mass balance. Examples will be given for each limiting type of solution behavior.

Keywords. Sulfate; Cryolite; Oxide solubility; Oxy-fluoride; Modeling.

Introduction

The thermodynamic description of equilibria in solutions is a subject with a long history and significant interest and importance. Among other fused salt systems, fused sulfate solutions and molten cryolite solutions have been extensively studied [1–7]. The former solutions are related to an important engineering problem: hot corrosion, *i.e.*, accelerated oxidation of high-temperature materials and coatings by a thin fused salt film. Alkali cryolite melts are associated with the electrowinning of primary aluminum by the *Hall-Heroult* process. In the 2000 TMS Institute of Metals Lecture, *Rapp* [8] generalized about equilibria in high-temperature ionic solutions, although his suggested analysis for treating cryolite solutions was incorrect, as explained in detail here.

Dissolved oxides in cryolite-base melts are known to form oxyfluoride complexes. Compositional variation in this system is made by varying the ''cryolite

[#] Dedicated to our friend and colleague Professor *Adolf Mikula* on the occasion of his 60th birthday

[*] Corresponding author. E-mail: rapp@matsceng.ohio-state.edu

ratio r'', defined as the molar ratio of NaF to AlF_3, with $r<3$ being an acidic melt and $r>3$ basic. In the NaF–AlF_3 system, the melt basicity, defined as $\log a_{NaF}$, can be established quantitatively by the use of two sensors measuring independently the thermodynamic activities of sodium and aluminum [9]. In the dissolution of alumina in Na_3AlF_6 at 1300 K, three complex oxyfluoride solutes ($Al_2OF_6^{2-}$, $Al_2O_2F_4^{2-}$, and $Al_2O_2F_6^{4-}$) are formed in relative proportions which depend upon the cryolite ratio [9, 10]. Because of the propensity to form only complexed solutes, the total range of realizable basicity (variation in $\log a_{NaF}$) is only about one decade, as seen below. Therefore, melts of cryolite base are not susceptible to wide variations in acid-base property, nor can the basicity be manipulated importantly, *e.g.* to control the solubility of some oxide.

In this paper, modeling the equilibria for the dissolution of alumina in the cryolite solvent is summarized.

Modeling of Al_2O_3 Solubility in Cryolite Melts at 1300 K

Skybakmoen et al. [2] accurately measured the solubility of alumina in cryolite melts for melt compositions of $1.5 \leq$ cryolite ratio $r \leq 3$ in a temperature range from 1123 to about 1323 K. *Solheim* and *Sterten* [3] reported empirical equations describing the activities of NaF (a_1), AlF_3 (a_2), and Al_2O_3 (a_3) as a function of cryolite ratio r and the molar fraction of dissolved alumina (x_3) for this range of cryolite ratio. Table 1 presents several sets of values for x_3, a_1, and a_2 at 1300 K that were calculated for different values of cryolite ratio r. Some other values for the solubility of alumina and component activities in basic melts with cryolite ratio $r>3$ were measured experimentally by the present authors [9], and are also included in Table 1.

Table 1. Alumina solubility and component activity data for 1300 K

Equilibrium cryolite ratio r	Melt chemistry		Alumina solubility (x_3) molar fraction
	a_{NaF}	a_{AlF_3}	
1.5	0.0564	1.998×10^{-2}	0.054
1.75	0.0993	8.192×10^{-3}	0.0622
2.0	0.1501	3.791×10^{-3}	0.0674
2.25	0.2032	1.980×10^{-3}	0.0704
2.5	0.2556	1.132×10^{-3}	0.0722
2.75	0.3072	6.848×10^{-4}	0.0736
3.0	0.3584	4.281×10^{-4}	0.075
3.58[a]	0.459	1.56×10^{-4}	0.080
4.10[a]	0.536	8.64×10^{-5}	0.081
4.65[a]	0.606	5.17×10^{-5}	0.079
5.25[a]	0.664	3.25×10^{-5}	0.077
6.42[a]	0.731	1.61×10^{-5}	0.073
8.44[a]	0.802	7.11×10^{-6}	0.062
12.5[a]	0.879	2.80×10^{-6}	0.048

[a] These data were measured and reported by the present authors [9]

Na_3AlF_6 and $NaAlF_4$ (denoted as C and E, respectively) are generally accepted as dominant anions for the solvent $NaF–AlF_3$ system. A questionable solute Na_2AlF_5 has also been proposed by some authors [11–13]. However, Na_2AlF_5 is unlikely to exist in these melts because of an unfavorable molecular geometry (stereochemistry) [10]. Therefore, the reaction equilibria in the $NaF–AlF_3$ system are described as shown by Eqs. (1) and (2).

$$3NaF(l) + AlF_3(s) = Na_3AlF_6(l)\ (C) \quad K_C \tag{1}$$

$$NaF(l) + AlF_3(s) = NaAlF_4(l)\ (E) \quad K_E \tag{2}$$

As described in a previous paper [9], acidic, neutral, and basic solutes $Na_2Al_2OF_6$, $Na_2Al_2O_2F_4$, and $Na_4Al_2O_2F_6$ (denoted as A, N, and B, respectively) were interpreted to be the oxyfluoride complexes responsible for the dissolution of alumina in the cryolite melts (Eqs. (3)–(5)).

$$\frac{1}{3}Al_2O_3(s) + 2NaF(l) + \frac{4}{3}AlF_3(s) = Na_2Al_2OF_6(l)\ (A) \quad K_A \tag{3}$$

$$\frac{2}{3}Al_2O_3(s) + 2NaF(l) + \frac{2}{3}AlF_3(s) = Na_2Al_2O_2F_4(l)\ (N) \quad K_N \tag{4}$$

$$\frac{2}{3}Al_2O_3(s) + 4NaF(l) + \frac{2}{3}AlF_3(s) = Na_4Al_2O_2F_6(l)\ (B) \quad K_B \tag{5}$$

The equilibrium constants for Eqs. (1)–(5) can be written in terms of the activities of the respective constituents for each reaction (Eqs. (1′)–(5′)), where a_1, a_2, and a_3 are the activities of NaF, AlF_3, and Al_2O_3, respectively.

$$[C] = K_C {a_1}^3 a_2 \tag{1'}$$

$$[E] = K_E a_1 a_2 \tag{2'}$$

$$[A] = K_A {a_1}^2 {a_2}^{4/3} {a_3}^{1/3} \tag{3'}$$

$$[N] = K_N {a_1}^2 {a_2}^{2/3} {a_3}^{2/3} \tag{4'}$$

$$[B] = K_B {a_1}^4 {a_2}^{2/3} {a_3}^{2/3} \tag{5'}$$

The activities of the solute unknowns in Eqs. (1′)–(5′) have been set equal to their molar fractions. Formally, this procedure implies a Henrian choice of standard state, *i.e.*, in the limit of infinite dilution, where each dilute solute has a constant activity coefficient, the activity is set equal to the molar fraction.

The activity of alumina is taken as unity in the α-Al_2O_3 stability range while in the β-Al_2O_3 stability range, *i.e.*, cryolite ratio $r > 3.69$ [9], the activity values for α-Al_2O_3 in Eqs. (1′)–(5′) were calculated from the following Eq. (6) [14].

$$2NaF(l) + \frac{34}{3}Al_2O_3(\alpha) = Na_2O \cdot 11Al_2O_3(\beta) + \frac{2}{3}AlF_3(s) \tag{6}$$

Sets of equations including the unknown equilibrium constants are established for combinations of all these solutes by means of element balances. For oxygen (Eq. (7)), where x_3 is the molar fraction of dissolved Al_2O_3 in a ternary system of

$NaF–AlF_3–Al_2O_3$, as listed in the last column in Table 1, and n_t is the total moles of all the species in the melt.

Other equations can similarly express element balances. For the Na elemental balance, Eq. (8), for the Al elemental balance, Eq. (9), and for the F elemental balance, Eq. (10).

$$([A] + 2[N] + 2[B])n_t = 3x_3 \tag{7}$$

$$(2[A] + 2[N] + 4[B] + 3[C] + [E] + [NaF])n_t = \frac{r}{r+1}(1 - x_3) \tag{8}$$

$$(2[A] + 2[N] + 2[B] + [C] + [E] + [AlF_3])n_t = \frac{1 + (2r+1)x_3}{r+1} \tag{9}$$

$$(6[A] + 4[N] + 6[B] + 6[C] + 4[E] + [NaF] + 3[AlF_3])n_t = \frac{r+3}{r+1}(1 - x_3) \tag{10}$$

In addition to these elemental balances, the sum of molar fractions for all the solutes should be unity for each composition of the cryolite melt (Eq. (11)).

$$[A] + [N] + [B] + [C] + [E] + [NaF] + [AlF_3] = 1 \tag{11}$$

These equations were solved simultaneously by the least-squares, data-fitting software program of Mathcad. This program provided minimum errors for all the relations described above; the largest deviation was less than 5%. The calculated equilibrium constants for the Eqs. (1)–(5) at 1300 K have the following values: $K_A = 13820$, $K_N = 386$, $K_B = 596$, $K_C = 16200$, and $K_E = 484$. Similar modeling assuming several sets of different proposed solutes resulted in much higher least-squares deviations.

Figure 1 shows a comparison of the experimentally determined alumina solubility in the $NaF–AlF_3$ system at 1300 K and the solubility calculated using the present model. In Fig. 1, the solubility of alumina is plotted as a function of

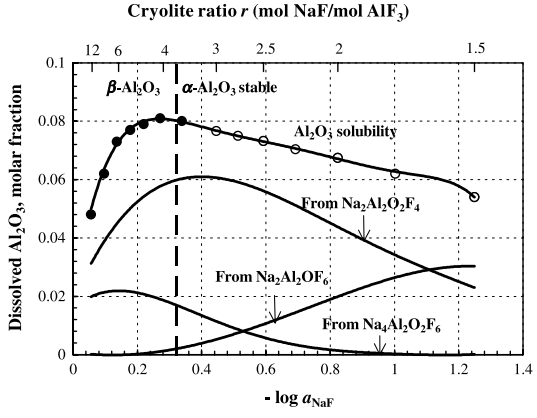

Fig. 1. Comparison of Al_2O_3 solubility in $NaF–AlF_3$ system at 1300 K as a function of melt basicity from experiments (data points) and calculated from the present model (top line); the other three lines represent the individual Al_2O_3 solubility contributions by acidic ($Na_2Al_2OF_6$), neutral ($Na_2Al_2O_2F_4$), and basic ($Na_4Al_2O_2F_6$) solutes, respectively

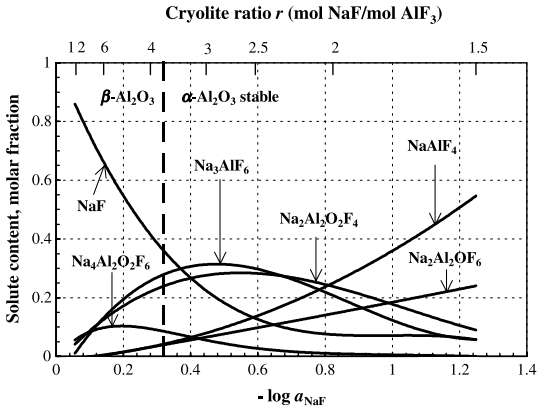

Fig. 2. Calculated concentrations of all solutes for an alumina-saturated cryolite melt at 1300 K

$-\log a_{NaF}$, with the corresponding values for cryolite ratio r also shown as an alternate abscissa. The solubility lines from the experimental measurements and from the modeling overlap each other, so the modeled alumina solubility is shown as a solid line, with data points indicating the experimentally measured solubility of alumina. The other three lines in Fig. 1 indicate the calculated dissolved alumina contents contributed by the acidic, neutral, and basic solutes: $Na_2Al_2OF_6$, $Na_2Al_2O_2F_4$, and $Na_4Al_2O_2F_6$, respectively. From Fig. 1, the melt basicity variation ($\log a_{NaF}$) realizable for the cryolite melt composition range of $1.5 \leq r \leq 12.5$ is only about one order of magnitude because the melt is buffered by the formation of complex anions.

The concentrations of all the complex solutes in the cryolite melts for $1.5 \leq r \leq 12.5$ were calculated according to the present model, and these results are plotted in Fig. 2. In this case, the molar fractions refer to the solution comprising six solutes, which sum to unity.

Extension of the Methodology to Cryolite Melts with Other Components at 1300 K

Once the equilibrium constants for formation of the species A, N, B, C, and E have been established, as just demonstrated, these constants can be considered as known quantities for a similar analysis of systems involving more components.

Jentoftsen, *Lorentsen*, *Dewing*, *Haarberg*, and *Thonstad* [15, 16] measured the solubilities of NiO and $NiAl_2O_4$ in an oxygen atmosphere and the solubilities of FeO and $FeAl_2O_4$ in a reducing atmosphere in cryolite melts at 1293 K. These authors used the traditional log–log methodology to discuss the dissolution mechanisms. They suggested that a single dominant solute species Na_3NiF_5 is responsible for dissolution of $NiAl_2O_4$ in Al_2O_3-saturated melts over the entire composition range investigated. In the case of $FeAl_2O_4$, they failed to identify the Fe-containing solute species in the melt. In fact, the log–log method of thermodynamic modeling is only effective when indeed a single solute species is dominant over a specific range of melt composition. However, cryolite melts are inherently highly buffered ionic solutions comprising several competitive complex

anions. In addition, any realistic solute in ionic solutions should also exhibit a reasonable anion geometry (stereochemistry), such as an tetrahedron or octahedron, *etc.*, so the anion solute NiF_5^{3-} cannot be considered as a realistic species.

A model involving two basic solutes of Na_2NiF_4 and Na_4NiF_6, and a model including an acidic solute of FeF_2 and two basic solutes of Na_2FeF_4 and Na_4FeF_6, were proposed by the present authors to explain the solubility behavior for $NiO/NiAl_2O_4$ and $FeO/FeAl_2O_4$, respectively [17]. Figures 3 and 4 show the

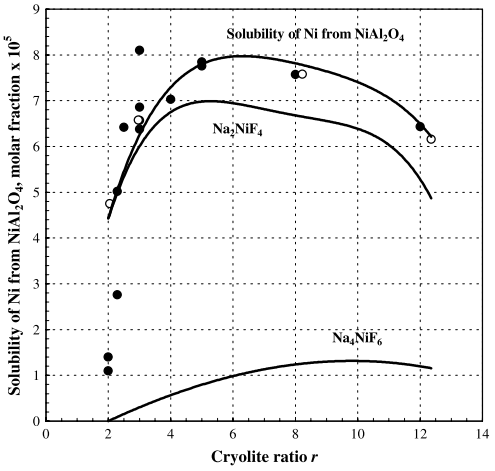

Fig. 3. Comparison of the experimentally determined solubility of Ni from $NiAl_2O_4$ in Al_2O_3-saturated cryolite melts at 1300 K and that calculated from the present model; the top solid line is the modeled $NiAl_2O_4$ solubility line, and the data points are experimentally determined values (solid circles from *Jentoftsen et al.* [15, 16] and open circles from the present authors [17]); the other two lines present the contributions from the two solutes Na_2NiF_4 and Na_4NiF_6, respectively

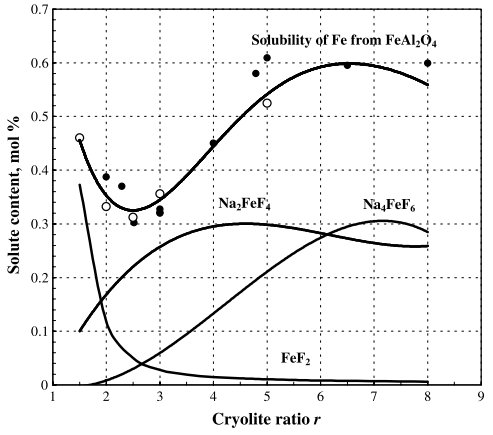

Fig. 4. Comparison of the experimentally determined solubility of Fe from $FeAl_2O_4$ in Al_2O_3-saturated cryolite melts at 1300 K and that calculated from the present model; the top solid line is the modeled Fe (from $FeAl_2O_4$) solubility line, and the data points are experimentally determined values (the solid circles are from *Jentoftsen et al.* [15, 16] and open circles from the present authors [17]); the other three lines present the contributions from the three solutes FeF_2, Na_2FeF_4, and Na_4FeF_6, respectively

modeled results. In these two figures, the experimentally measured solubility data points for Ni from $NiAl_2O_4$ and Fe from $FeAl_2O_4$, respectively, in Al_2O_3-saturated cryolite melts at 1300 K are in good agreement with the calculated modeling lines. In addition, the anion solutes NiF_4^{2-}, NiF_6^{4-}, FeF_4^{2-}, and FeF_6^{4-} exhibit simple geometries, either tetrahedra or octahedra. The extension of the modeling analysis to these other systems was made possible only because the equilibrium constants for the formation of the five complex anions in the Na–Al–O–F system were known from the previous study.

Similar modeling of the TiO_2 solubility in cryolite-alumina melts at 1300 K was also undertaken by the present authors [18].

Concluding Remarks

Unlike a fully ionized sodium sulfate solution, an inherently highly buffered ionic solution such as a cryolite-base melt does not exhibit individual solutes of oxides that dominate over a wide solution composition range. Therefore, the classical log–log method to achieve thermodynamic modeling cannot be effective. Rather, the several competitive complex solutes must be identified by fitting the experimental data to multiple equilibria. In this way, the stabilities (standard *Gibbs* formation energies based on Henrian standard states) for the solutes are also determined. The solute species identified by the present authors for Al_2O_3 in cryolite melts, and the solutes for $NiO/NiAl_2O_4$ in cryolite-Al_2O_3 melts, and for $FeO/FeAl_2O_4$ in cryolite-Al_2O_3 melts not only provide the best fit to the experimentally measured solubility data but also exhibit reasonable 3-D anion geometries.

Acknowledgements

This research was sponsored by the Department of Energy (DOE-OIT Project No. DE-FC07-99ID 13813, *J. Yankeelov*, Project Monitor).

References

[1] Rapp RA, Zhang YS (1994) JOM **46**: 47
[2] Skybakmoen E, Solheim A, Sterten A (1997) Metall Mater Trans B **28B**: 81
[3] Solheim A, Sterten A (1999) Light Metals 1999, TMS, Warrendale, PA, p 445
[4] Dewing EW (1990) Metall Trans B **21B**: 285
[5] Kvande H (1986) Light Metals 1986, TMS, Warrendale, PA, p 451
[6] Gilbert B, Robert E, Tixhon E, Olsen JE, Ostvold T (1995) Light Metals 1995, TMS, Warrendale, PA, p 181
[7] Danek V, Gustarsen OT, Ostvold T (2000) Can Met Q **39**: 153
[8] Rapp RA (2000) Metall Mater Trans A **31A**: 2105
[9] Zhang YS, Wu X, Rapp RA (2003) Metall Mater Trans B **34B**: 235
[10] Zhang YS, Rapp RA (2004) Metall Mater Trans B **35B**: 509
[11] Dewing EW (1986) Proceedings of the 5th International Symposium on Molten Salts (Edited by Saboungi ML, Newman DS, Johnson K, Inman D). The Electrochem. Soc. Inc., Pennington, NJ, p 262
[12] Gilbert B, Robert E, Tixhon E, Olsen JE, Ostvold T (1996) Inorg Chem **35**: 4198
[13] Gilbert B, Materne T (1990) Appl Spectr **44**: 299

[14] Sterten A, Hamberg K, Maeland I (1982) Acta Chem Scand A **36**: 329
[15] Jentoftsen TE, Lorentsen OA, Dewing EW (2001) Light Metals 2001, TMS, Warrendale, PA, p 455
[16] Jentoftsen TE, Lorentsen OA, Dewing EW, Haarberg GM, Thonstad J (2002) Metall Mater Trans B **35B**: 182
[17] Zhang YS, Wu X, Rapp RA (2004) Metall Mater Trans B **35B**: 133
[18] Zhang YS, Rapp RA (2004) Metall Mater Trans B **35B**: 183